Trends in Clinical and Medical Sciences

PSR Press

Article

Control-dependent reproduction numbers for acute viral conjunctivitis: A corrected SEIR threshold analysis

Vianney Mbazumutima[1,*], Charline Uwilingiyimana[2], Pascaline Nshimirimana[1], Heri Retnawati[3], Justin Ushize Rutikanga[4] and Léonard Todjihounde[5]

[1] Department of Natural Sciences, École Normale Supérieure du Burundi, Boulevard du 28 Novembre, P.O. Box 6983, Bujumbura, Burundi
[2] Department of Statistics Applied to Economy, Faculty of Sciences and Information Technology, INES-Ruhengeri–Institute of Applied Sciences, NM 155 Street, P.O. Box 155, Ruhengeri, Rwanda
[3] Department of Educational Research and Evaluation, Universitas Negeri Yogyakarta, Jl. Colombo No. 1, Karangmalang, Yogyakarta 55281, Indonesia
[4] Department of Agricultural Mechanization, School of Agricultural Engineering, College of Agriculture, Forestry and Food Sciences (CAFF), University of Rwanda, Busogo Campus, P.O. Box 210, Musanze, Rwanda
[5] Department of Mathematics, Institut de Mathématiques et de Sciences Physiques (IMSP), Université d'Abomey-Calavi, Dangbo, 01 B.P. 613, Porto-Novo, Republic of Bénin
* Correspondence: vianney.mbazumutima@imsp-uac.org

Received: 24 June 2026; Accepted: 19 August 2026; Published: 14 September 2026.

Abstract: Acute viral conjunctivitis can generate rapidly growing outbreaks in schools and other close-contact settings, but intervention comparisons are meaningful only when the underlying transmission model is dimensionally consistent and its reproduction numbers are reproducible. We formulate a closed-population susceptible–exposed–infectious–recovered (SEIR) model with two distinct controls: a dimensionless reduction in effective contact, u_1, and treatment-supported case management, u_2, which increases removal from infectious contact at a maximum rate τ. The basic reproduction number is $R_0 = \beta/\gamma$, the controlled invasion number is $R_c = \beta(1-u_1)/(\gamma+\tau u_2)$, and the state-dependent effective reproduction number is $R_e(t) = R_c S(t)/N$. These expressions satisfy the required identity $R_c(0,0) = R_0$ and yield an explicit control threshold. The baseline scenario is calibrated to the published estimate $R_0 = 2.64$ for acute haemorrhagic conjunctivitis, with a 1.5-day latent period and a 5-day infectious period. Contact reduction alone crosses the invasion threshold at $u_1 = 0.621$, whereas the assumed case-management range does not do so alone. A combined scenario $(u_1, u_2) = (0.50, 0.80)$ gives $R_c = 0.660$ and limits new infections to 0.289% of initially susceptible individuals in a 10,000-person illustrative cohort, compared with 90.938% without control. A 10,000-draw uncertainty analysis gives a 93.9% probability that the combined scenario maintains $R_c < 1$. Independent numerical solvers agree to within 4.4×10^{-10} persons, and population is conserved to within 7.7×10^{-11} persons. The results support combined intervention thresholds as transparent scenario analyses; they do not constitute a clinical ranking of treatments or a population-specific forecast without local calibration.

Keywords: acute viral conjunctivitis, SEIR model, controlled reproduction number, effective reproduction number, contact reduction, case management, uncertainty analysis

1. Introduction

Viral conjunctivitis is a common cause of infectious red eye and encompasses clinically and epidemiologically distinct conditions. Adenoviruses account for a large share of viral conjunctivitis, while acute haemorrhagic conjunctivitis (AHC) is commonly associated with enterovirus 70 and coxsackievirus A24 variant [1,2]. AHC is especially relevant to outbreak modeling because it has a short incubation period, high transmissibility, and the capacity to spread rapidly in schools and other settings with frequent close contact [3–5]. These features make early contact reduction, hygiene, surveillance, diagnosis, and removal from infectious contact plausible components of outbreak control.

Previous mathematical studies have examined conjunctivitis transmission using compartmental models, quarantine, isolation, treatment, education, and optimal-control formulations [4,6–9]. This literature demonstrates the value of mathematical thresholds, but it also shows why intervention parameters must be clearly defined. A dimensionless reduction in contact cannot be compared directly with a removal rate unless their mechanisms, units, and admissible ranges are specified. Likewise, a controlled reproduction number evaluated at a disease-free state is not identical to a time-dependent effective reproduction number, which also depends on the susceptible fraction.

The present study addresses these issues with four contributions. First, it uses a closed-population SEIR outbreak model whose incidence and transition terms are dimensionally consistent and whose feasible region is positively invariant. Second, it derives the basic, controlled, and state-dependent effective reproduction numbers from the infected subsystem using the next-generation-matrix method [10,11]. Third, it identifies the complete threshold curve separating invasion from decline under contact reduction and treatment-supported case management. Fourth, it evaluates representative intervention scenarios with reproducible ordinary differential equation simulations, a 10,000-draw parameter uncertainty analysis, mass-balance tests, and cross-solver numerical verification.

The analysis is deliberately framed as an outbreak scenario rather than an empirical forecast for a particular country. The baseline transmissibility and natural-history values are anchored to published AHC estimates [3], whereas the maximum additional removal rate attributable to case management is treated as an explicit scenario parameter and varied over a broad range. This separation prevents an assumed operational parameter from being presented as a measured clinical effect.

2. Materials and methods

2.1. Conjunctivitis model without control measures

Let $S(t)$, $E(t)$, $I(t)$, and $R(t)$ denote the numbers of susceptible, exposed but not yet infectious, infectious, and removed individuals at time t, respectively. The total population is

$$N = S(t) + E(t) + I(t) + R(t).$$

Because acute conjunctivitis outbreaks typically unfold over weeks rather than decades, births, natural deaths, and waning immunity are omitted. This short-horizon assumption avoids introducing demographic rates that are neither identifiable nor influential on the outbreak time scale. Homogeneous mixing is assumed, and all exposed individuals eventually become infectious. Figure 1 summarizes the transitions.

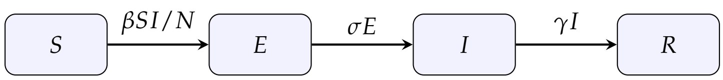

Figure 1. Flow diagram of the uncontrolled acute viral conjunctivitis SEIR model

The corresponding equations are

$$\begin{cases} \frac{dS}{dt} &= -\beta\frac{SI}{N}, \\ \frac{dE}{dt} &= \beta\frac{SI}{N} - \sigma E, \\ \frac{dI}{dt} &= \sigma E - \gamma I, \\ \frac{dR}{dt} &= \gamma I. \end{cases} \tag{1}$$

Here β is the effective transmission coefficient, σ^{-1} is the mean latent period, and γ^{-1} is the mean duration of infectious contact. Every term in Eq. (1) has units of persons per day.

Adding the equations gives

$$\frac{d}{dt}(S + E + I + R) = 0, \tag{2}$$

so $N(t) = N(0) = N$. On any coordinate boundary, the derivative of the corresponding compartment is nonnegative: for example, $dE/dt = \beta SI/N \geq 0$ when $E = 0$, and $dI/dt = \sigma E \geq 0$ when $I = 0$. Therefore the biologically feasible region

$$\Omega = \left\{ (S, E, I, R) \in \mathbb{R}_+^4 : S + E + I + R = N \right\}, \tag{3}$$

is positively invariant, and all solutions beginning in Ω remain nonnegative and bounded. The infection-free state used for invasion analysis is

$$\mathcal{E}_0 = (N, 0, 0, 0). \tag{4}$$

In a closed outbreak model there is no demographic endemic equilibrium with a constant positive infectious population; instead, the epidemic terminates on the infection-free set $E = I = 0$ after susceptible depletion and removal.

Table 1 lists the baseline values. Chowell et al. estimated that a primary infectious AHC case generated approximately 2.64 secondary cases, with standard deviation 0.65, in the 2003 Mexico outbreak [3]. The same outbreak literature reports an incubation period of approximately 1–2 days and an infectious period of approximately 3–7 days; their midpoints give $\sigma = 1/1.5 = 0.6667$ day^{-1} and $\gamma = 1/5 = 0.2000$ day^{-1}. We set $\beta = R_0\gamma = 0.5280$ day^{-1}. The value $\tau = 0.25$ day^{-1} is an operational scenario assumption, not a drug-efficacy estimate, and is varied from 0.15 to 0.35 day^{-1} in uncertainty analysis.

Table 1. Baseline parameters and simulation quantities

Symbol	Interpretation	Baseline value	Units or source
N	Size of the illustrative closed cohort	10,000	persons; scenario
β	Effective transmission coefficient	0.5280	day^{-1}; calibrated from [3]
σ	Progression rate from exposed to infectious	0.6667	day^{-1}; 1.5-day mean [3]
γ	Baseline removal rate from infectious contact	0.2000	day^{-1}; 5-day mean [3]
τ	Maximum additional removal rate under case management	0.2500	day^{-1}; scenario range 0.15–0.35
u_1	Proportional reduction in effective contact	$[0, 1]$	dimensionless control
u_2	Intensity of treatment-supported case management	$[0, 1]$	dimensionless control

2.2. Basic reproduction number

The infected-state vector is $x = (E, I)^\top$. At $\mathcal{E}_0$, the new-infection and transition matrices are

$$F = \begin{pmatrix} 0 & \beta \\ 0 & 0 \end{pmatrix}, \qquad V = \begin{pmatrix} \sigma & 0 \\ -\sigma & \gamma \end{pmatrix}. \tag{5}$$

Thus

$$FV^{-1} = \begin{pmatrix} \beta/\gamma & \beta/\gamma \\ 0 & 0 \end{pmatrix}, \qquad R_0 = \rho(FV^{-1}) = \frac{\beta}{\gamma}. \tag{6}$$

The latent rate σ does not appear in R_0 because, under the stated assumptions, every exposed individual survives the latent stage and enters the infectious class. Substituting the baseline values gives $R_0 = 0.5280/0.2000 = 2.64$, consistent by construction with the published AHC estimate.

2.3. Conjunctivitis model with control measures

Two controls are distinguished mechanistically. The contact-reduction control $u_1 \in [0, 1]$ is the proportional decrease in effective infectious contacts associated with measures such as hand hygiene, environmental disinfection, reduced close contact, and adherence to separation guidance. The case-management control $u_2 \in [0, 1]$ represents prompt identification and treatment-supported removal from infectious contact. It is not interpreted as a direct antiviral cure. Its maximum additional removal rate is τ, so its dimensional contribution is τu_2 day^{-1}. Figure 2 shows the controlled flows.

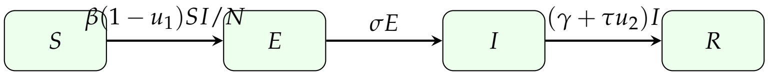

Figure 2. Flow diagram of the controlled model. The two controls act through different, dimensionally explicit mechanisms

The controlled system is

$$\begin{cases} \frac{dS}{dt} &= -\beta(1-u_1)\frac{SI}{N}, \\ \frac{dE}{dt} &= \beta(1-u_1)\frac{SI}{N} - \sigma E, \\ \frac{dI}{dt} &= \sigma E - (\gamma + \tau u_2)I, \\ \frac{dR}{dt} &= (\gamma+\tau u_2)I. \end{cases} \tag{7}$$

The conservation and positivity arguments used for the uncontrolled system remain valid for every admissible pair $(u_1, u_2) \in [0,1]^2$.

2.4. Controlled and effective reproduction numbers

For constant control levels, the next-generation construction applied to Eq. (7) gives

$$F_c = \begin{pmatrix} 0 & \beta(1-u_1) \\ 0 & 0 \end{pmatrix}, \qquad V_c = \begin{pmatrix} \sigma & 0 \\ -\sigma & \gamma+\tau u_2 \end{pmatrix}, \tag{8}$$

and hence

$$R_c(u_1,u_2) = \rho(F_c V_c^{-1}) = \frac{\beta(1-u_1)}{\gamma+\tau u_2}. \tag{9}$$

The required consistency identity follows immediately:

$$R_c(0,0) = \frac{\beta}{\gamma} = R_0.$$

The state-dependent effective reproduction number is

$$R_e(t; u_1, u_2) = R_c(u_1,u_2)\frac{S(t)}{N}. \tag{10}$$

Unlike R_c, which is an invasion threshold at the fully susceptible state, $R_e(t)$ decreases as susceptible individuals are removed.

The Jacobian of the infected subsystem (E, I) at $\mathcal{E}_0$ has characteristic polynomial

$$\lambda^2 + (\sigma+\gamma+\tau u_2)\,\lambda + \sigma\,(\gamma+\tau u_2)\,[1 - R_c(u_1,u_2)] = 0. \tag{11}$$

Both Routh–Hurwitz coefficients are positive when $R_c < 1$, so the infection-free state is locally asymptotically stable in the infected directions. When $R_c > 1$, the constant term is negative and one eigenvalue is positive; invasion is then possible.

Solving $R_c = 1$ gives the threshold curve

$$u_{1,\mathrm{crit}}(u_2) = \max\left\{0,\, 1 - \frac{\gamma+\tau u_2}{\beta}\right\}. \tag{12}$$

Equivalently, for a fixed u_1, case management must satisfy

$$u_2 > \frac{\beta(1-u_1)-\gamma}{\tau},$$

whenever the right-hand side is positive.

3. Results and discussion

3.1. Numerical simulations

The controlled system was solved over 120 days for an illustrative cohort of $N = 10{,}000$ with

$$(S(0), E(0), I(0), R(0)) = (9985, 10, 5, 0).$$

The primary calculations used the DOP853 method with relative tolerance 10^{-10}, absolute tolerance 10^{-12}, and maximum internal step 0.05 day. Recalculation with RK45, tighter reference tolerances, and a 0.025-day maximum step was used for numerical verification. The complete Python script, random seed, PNG files, and numerical summaries accompany the manuscript.

Figure 3(a) shows that case management alone decreases R_c monotonically from 2.64 at $u_2 = 0$ to 1.173 at $u_2 = 1$. Under the assumed maximum additional removal rate, it cannot reduce the invasion number below one by itself. This does not mean that case management is ineffective: it reduces the simulated peak and attack rate substantially, but its baseline parameterization is insufficient for prevention of invasion when used alone. Figure 3(b) shows the linear effect of contact reduction. The exact contact-only threshold is

$$u_{1,\text{crit}}(0) = 1 - \frac{1}{R_0} = 0.6212.$$

Therefore $u_1 > 0.6212$ gives $R_c < 1$ at the baseline parameter values.

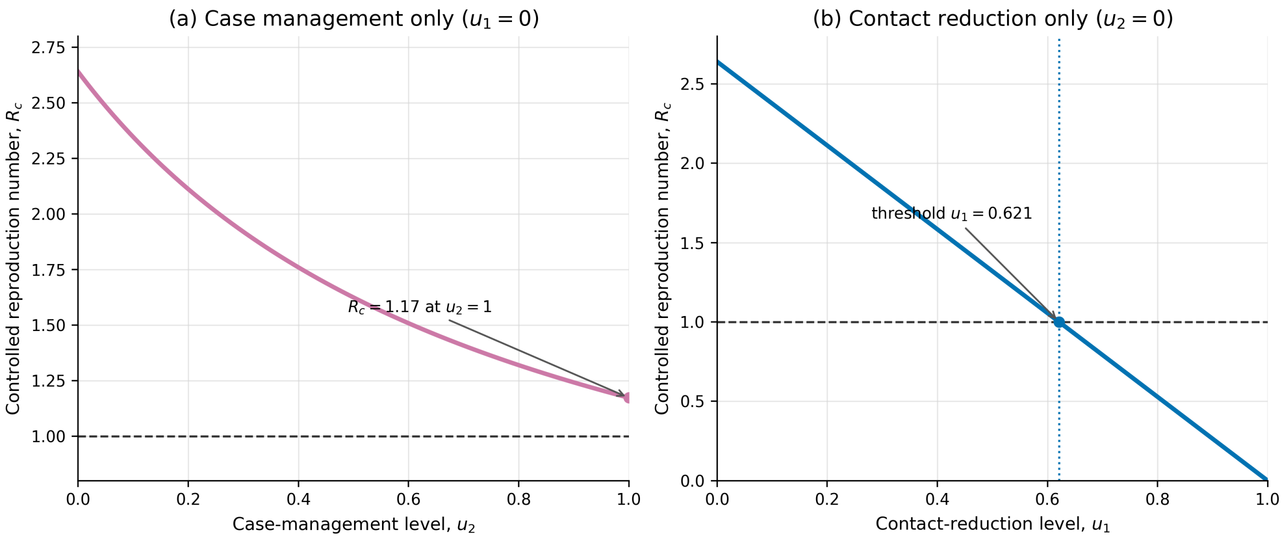

Figure 3. Controlled reproduction number under a single active control. (a) Case management varies while $u_1 = 0$. (b) Contact reduction varies while $u_2 = 0$. The horizontal dashed line marks $R_c = 1$

Four dynamic scenarios were examined: no control $(0, 0)$; contact reduction only $(0.65, 0)$; case management only $(0, 0.80)$; and combined controls $(0.50, 0.80)$. Their controlled reproduction numbers are 2.640, 0.924, 1.320, and 0.660, respectively. As shown in Figure 4(a), the uncontrolled scenario peaks at 1934.952 infectious individuals on day 34.45 and generates new infections in 90.938% of initially susceptible individuals by day 120. Contact reduction alone produces a much smaller transient peak of 11.028 infectious individuals on day 4.40 and a 1.312% attack rate. Case management alone delays and reduces the epidemic, but because $R_c = 1.320 > 1$, it still produces a peak of 207.467 infectious individuals on day 60.45 and a 43.988% attack rate. The combined scenario gives a peak of 8.156 infectious individuals on day 1.95 and a 0.289% attack rate.

Figure 4(b) distinguishes the time-dependent $R_e(t)$ from the constant invasion value R_c. For the contact-only and combined scenarios, $R_e(t) < 1$ from the start. For the uncontrolled and case-management-only scenarios, susceptible depletion eventually pushes $R_e(t)$ below one, but only after substantial transmission. This timing explains why crossing below one late in an outbreak cannot be interpreted as successful early prevention.

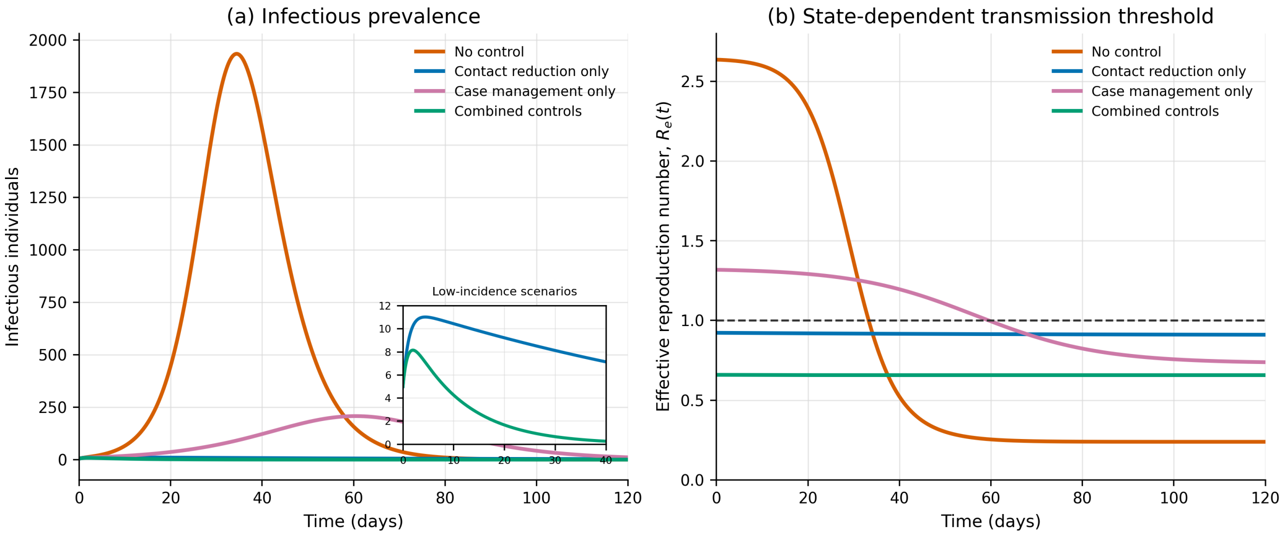

Figure 4. Dynamic simulations for four control scenarios. (a) Infectious prevalence, with an inset resolving the low-incidence scenarios. (b) The corresponding state-dependent effective reproduction number $R_e(t) = R_c S(t)/N$

Figure 5 displays R_c over the full admissible control square. The white contour is the analytic boundary from Eq. (12); points to its upper-right satisfy $R_c < 1$. At $u_2 = 0.80$, the minimum contact reduction required by the baseline parameters is $u_1 > 0.2424$. Conversely, at $u_1 = 0.50$, the minimum case-management level is $u_2 > 0.2560$. The selected combined point $(0.50, 0.80)$ lies well inside the $R_c < 1$ region and gives $R_c = 0.660$.

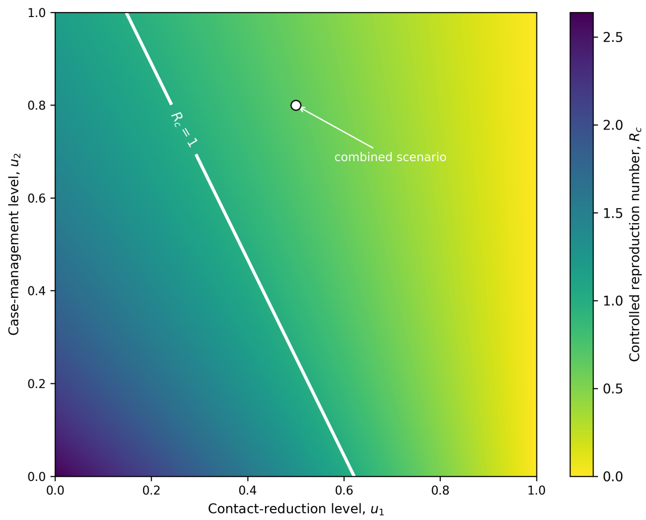

Figure 5. Heat map of the controlled reproduction number over contact-reduction and case-management levels. The white contour marks $R_c = 1$; the circle identifies the combined simulation scenario $(u_1, u_2) = (0.50, 0.80)$

Parameter uncertainty was evaluated with 10,000 Monte Carlo draws using the fixed random seed 20260725. The published reproduction-number estimate was represented by a normal distribution with mean 2.64 and standard deviation 0.65, truncated to $[1.1, 5.0]$; the infectious period was sampled uniformly from 3 to 7 days; and τ was sampled uniformly from 0.15 to 0.35 day^{-1}. For each draw, γ was the reciprocal of the sampled infectious period and $\beta = R_0\gamma$. The no-control median was 2.645 with a 95% simulation interval of 1.463–3.906. The contact-only scenario had median $R_c = 0.926$ (95% interval 0.512–1.367) and $P(R_c < 1) = 0.631$. The case-management-only scenario had median 1.322 (95% interval 0.679–2.215) and $P(R_c < 1) = 0.183$. The combined scenario had median 0.661 (95% interval 0.339–1.108) and $P(R_c < 1) = 0.939$. These intervals show that threshold conclusions close to one are sensitive to uncertain operational effectiveness; the combined strategy is more robust in this parameter space, but not guaranteed under every draw.

The numerical implementation passed three internal validation tests. First, $R_c(0,0) - R_0$ was zero to machine precision. Second, the maximum population-balance error across all scenarios was 7.64×10^{-11} persons, and no compartment became negative. Third, the maximum absolute difference between the DOP853 and RK45 solutions was 4.35×10^{-10} persons. These checks establish computational reproducibility and internal consistency, although they are not a substitute for validation against independent outbreak data.

The model has several limitations. Homogeneous mixing ignores household, classroom, age, and spatial structure. Controls are constant within each scenario, whereas adherence and implementation often change after outbreak recognition. The exposed class is assumed noninfectious, all exposed individuals progress to infectiousness, and the case-management rate τ is scenario-based rather than estimated from patient-level data. Environmental persistence and indirect transmission are absorbed into β rather than represented by a separate reservoir. Finally, the calibration is based on AHC evidence and should not be transferred without adjustment to adenoviral or other viral conjunctivitis syndromes with different natural histories. For application to a specific population, the model should be fitted to local onset data and accompanied by identifiable intervention dates, reporting corrections, and out-of-sample assessment.

4. Conclusion

A dimensionally consistent SEIR formulation yields clear distinctions among R_0, the controlled invasion number R_c, and the state-dependent effective number $R_e(t)$. Under the baseline AHC calibration, contact reduction alone crosses the invasion threshold at $u_1 = 0.621$, the assumed case-management range does not cross it alone, and the combined scenario $(0.50, 0.80)$ gives $R_c = 0.660$. Dynamic simulations, uncertainty analysis, mass conservation, and cross-solver agreement support the internal validity of these results. The findings indicate complementarity between contact reduction and prompt case management, rather than a universal ranking of one intervention above the other. Population-specific recommendations require local calibration and empirical estimates of intervention effectiveness.

Author Contributions: Conceptualization, V.M. and C.U.; methodology, V.M., H.R., J.U.R., and L.T.; software, V.M. and C.U.; investigation, P.N. and J.U.R.; writing—original draft preparation, V.M. and P.N.; writing—review and editing, P.N. and C.U.; visualization, V.M., J.U.R., and P.N.; supervision, H.R. and L.T. All authors have read and agreed to the submitted version of the manuscript.

Funding Information: This research received no external funding.

Conflicts of Interest: The authors declare no conflict of interest.

Data Availability: No new patient-level data were used. The complete simulation code, fixed random seed, generated PNG figures, scenario summaries, uncertainty output, and numerical validation results are included with the LaTeX source.

References

[1] Muto, T., Imaizumi, S., & Kamoi, K. (2023). Viral conjunctivitis. *Viruses, 15*(3), Article 676.

[2] Tavares, F. N., Costa, E. V., Oliveira, S. S., Nicolai, C. C. A., Baran, M., & da Silva, E. E. (2006). Acute hemorrhagic conjunctivitis and coxsackievirus A24v, Rio de Janeiro, Brazil, 2004. *Emerging Infectious Diseases, 12*(3), 495–497.

[3] Chowell, G., Shim, E., Brauer, F., Díaz-Dueñas, P., Hyman, J. M., & Castillo-Chavez, C. (2006). Modelling the transmission dynamics of acute haemorrhagic conjunctivitis: Application to the 2003 outbreak in Mexico. *Statistics in Medicine, 25*(11), 1840–1857.

[4] Chen, S. L., Liu, R. C., Chen, F. M., Zhang, X. X., Zhao, J., & Chen, T. M. (2017). Dynamic modelling of strategies for the control of acute haemorrhagic conjunctivitis outbreaks in schools in Changsha, China (2004–2015). *Epidemiology and Infection, 145*(2), 368–378.

[5] Zhang, S., Hu, Q., Deng, Z., Hu, S., Liu, F., Yu, S., Liu, R., He, C., Li, H., Gao, L., & Chen, T. (2020). Transmissibility of acute haemorrhagic conjunctivitis in small-scale outbreaks in Hunan Province, China. *Scientific Reports, 10*, Article 119.

[6] Chen, B., Ge, Y., Zhang, L., Zhang, Y., Zhong, Z., & Liu, X. (2014). A modeling and experiment framework for the emergency management in AHC transmission. *Computational and Mathematical Methods in Medicine, 2014*, Article 897532.

[7] Ogunmiloro, O. M. (2020). Stability analysis and optimal control strategies of direct and indirect transmission dynamics of conjunctivitis. *Mathematical Methods in the Applied Sciences, 43*(18), 10619–10636.

[8] Viriyapong, R., & Khedwan, N. (2019). Effects of isolation by taking sick leaves of conjunctivitis infected individuals and treatment control on stability of mathematical modeling of conjunctivitis. *Science, Engineering and Health Studies, 13*(1), 20–28.

[9] Mbazumutima, V., Nshimirimana, P., Dembélé, A., Ndayiragije, F., & Todjihounde, L. (2025). Mathematical modelling of conjunctivitis viral disease: Case of Burundi. *Open Journal of Applied Sciences, 15*(5), 1366–1377.

[10] Diekmann, O., Heesterbeek, J. A. P., & Metz, J. A. J. (1990). On the definition and the computation of the basic reproduction ratio R_0 in models for infectious diseases in heterogeneous populations. *Journal of Mathematical Biology, 28*(4), 365–382.

[11] van den Driessche, P., & Watmough, J. (2002). Reproduction numbers and sub-threshold endemic equilibria for compartmental models of disease transmission. *Mathematical Biosciences, 180*(1–2), 29–48.